Original Article | Thoracic Imaging

eISSN 2005-8330
https://doi.org/10.3348/kjr.2022.0295
Korean J Radiol 2022;23(9):921-930

Korean Journal of Radiology
KJR

Combination of ^{18}F-Fluorodeoxyglucose PET/CT Radiomics and Clinical Features for Predicting Epidermal Growth Factor Receptor Mutations in Lung Adenocarcinoma

Shen Li[1], Yadi Li[1], Min Zhao[2], Pengyuan Wang[1], Jun Xin[1]

[1]Department of Radiology, Shengjing Hospital of China Medical University, Shenyang, China; [2]Pharmaceutical Diagnostics, GE Healthcare, Beijing, China

Objective: To identify epidermal growth factor receptor (EGFR) mutations in lung adenocarcinoma based on ^{18}F-fluorodeoxyglucose (FDG) PET/CT radiomics and clinical features and to distinguish EGFR exon 19 deletion (19 del) and exon 21 L858R missense (21 L858R) mutations using FDG PET/CT radiomics.

Materials and Methods: We retrospectively analyzed 179 patients with lung adenocarcinoma. They were randomly assigned to training (n = 125) and testing (n = 54) cohorts in a 7:3 ratio. A total of 2632 radiomics features were extracted from the tumor region of interest from the PET (1316) and CT (1316) images. Six PET/CT radiomics features that remained after the feature selection step were used to calculate the radiomics model score (rad-score). Subsequently, a combined clinical and radiomics model was constructed based on sex, smoking history, tumor diameter, and rad-score. The performance of the combined model in identifying EGFR mutations was assessed using a receiver operating characteristic (ROC) curve. Furthermore, in a subsample of 99 patients, a PET/CT radiomics model for distinguishing 19 del and 21 L858R EGFR mutational subtypes was established, and its performance was evaluated.

Results: The area under the ROC curve (AUROC) and accuracy of the combined clinical and PET/CT radiomics models were 0.882 and 81.6%, respectively, in the training cohort and 0.837 and 74.1%, respectively, in the testing cohort. The AUROC and accuracy of the radiomics model for distinguishing between 19 del and 21 L858R EGFR mutational subtypes were 0.708 and 66.7%, respectively, in the training cohort and 0.652 and 56.7%, respectively, in the testing cohort.

Conclusion: The combined clinical and PET/CT radiomics model could identify the EGFR mutational status in lung adenocarcinoma with moderate accuracy. However, distinguishing between EGFR 19 del and 21 L858R mutational subtypes was more challenging using PET/CT radiomics.

Keywords: *PET/CT; Radiomics; Epidermal growth factor receptor; Lung adenocarcinoma; Prediction*

INTRODUCTION

Lung cancer is a malignant tumor with the highest morbidity and mortality rates worldwide [1] with a 5-year survival rate of approximately 20% [2]. Lung adenocarcinoma accounts for nearly 40% of all lung cancer cases [3]. The early symptoms of lung adenocarcinoma are insidious, and most patients miss the opportunity to undergo radical surgery at the time of consultation. Epidermal growth factor receptor (EGFR) mutations are the most common genetic mutations in lung adenocarcinoma [4]. Patients with EGFR mutations can be treated with targeted tyrosine kinase inhibitors (TKIs), such as afatinib and erlotinib [5]. Previous studies have shown that TKIs can prolong the disease-free and overall survivals of patients with EGFR mutations [6-8]. Exon 19 deletion (19

Received: February 19, 2022 **Revised:** June 22, 2022 **Accepted:** June 27, 2022
Corresponding author: Jun Xin, MD, PhD, Department of Radiology, Shengjing Hospital of China Medical University, No. 36 Sanhao Street, Heping District, Shenyang 110004, China.
• E-mail: xinj@sj-hospital.org

del) and exon 21 L858R missense (21 L858R) account for approximately 85%–90% of all EGFR mutational types [9], and afatinib or oxitinib is clinically preferred for patients with 19 del, whereas erlotinib, in conjunction with bevacizumab, is recommended for patients with 21 L858R. Therefore, it is vital to clarify whether lung adenocarcinoma is accompanied by EGFR mutations and their exact mutational subtypes before targeted therapy.

An analysis of tumor tissues acquired by biopsy or surgical excision is the gold standard for diagnosing EGFR mutations; however, these tests are invasive. Surgery for central lung adenocarcinoma is risky, and a risk of secondary puncture surgery exists owing to the presence of heterogeneous or necrotic tumor tissue. Moreover, the false-negative rate of circulating tumor DNA for EGFR mutation detection is high, and the detection is expensive [10,11]. Therefore, a noninvasive and efficient diagnostic method is required.

^{18}F-fluorodeoxyglucose (^{18}F-FDG) PET/CT has been widely used for the diagnosis and staging of cancers [12,13]. EGFR mutations activate multiple signaling pathways that indirectly affect the tumor glucose uptake [14]. Some researchers have reported that the maximum standardized uptake value (SUVmax) of EGFR-mutant tumors is lower than that of EGFR wild-type tumors (both $p < 0.001$) [15,16]; however, Caicedo et al. [17] suggested no statistical difference in the SUVmax between these two types ($p = 0.742$). This inconsistent result indicates that the metabolic parameters of PET/CT are not stable enough to predict the EGFR mutational status. With the rapid development of radiomics, many researchers have attempted to use it to discriminate the EGFR mutational status [18]. Based on PET/CT radiomics features, it is not only possible to quantify the characteristics and change patterns of pixel grayscale distribution but also to reveal the heterogeneity of ^{18}F-FDG spatial distribution, thus reflecting the subtle differences between different tumors [19]. As previously reported, a diagnostic model based on PET/CT radiomics features can identify EGFR mutational status [20,21]; however, the reliance on radiomics alone is one-sided. Moreover, few studies have identified EGFR mutational subtypes using radiomics. Therefore, this study aimed to integrate PET/CT radiomics and clinical features to identify the EGFR mutational status in patients with lung adenocarcinoma. Additionally, to guide individualized treatment plans more precisely, we constructed a PET/CT radiomics model to distinguish between the 19 del and 21 L858R EGFR mutational subtypes.

MATERIALS AND METHODS

Patients

This retrospective study was approved by the Ethics Committee of Shengjing Hospital of China Medical University (IRB No. 2021PS686K). Informed consent was obtained from all the patients. A total of 179 patients were enrolled between January 2015 and October 2021. The inclusion criteria were as follows: 1) no antitumor treatment before PET/CT examination, 2) EGFR genetic testing within one month before and after PET/CT examination, 3) lung adenocarcinoma confirmed by pathological examination, and 4) a single tumor lesion with a diameter greater than 1 cm. The exclusion criteria were as follows: 1) combined with other malignant tumors (n = 3), and 2) unclear tumor boundaries (n = 17), hindering the accurate outlining of the region of interest (ROI). Among the 179 patients, 74 had the wild-type EGFR genotype and 105 had EGFR mutations (EGFR exon 18 mutations: n = 3; exon 19 del mutations: n = 46; exon 21 L858R mutations: n = 53; exon 21 L861Q mutations: n = 3). These patients were randomly divided into training (n = 125) and testing (n = 54) cohorts in a 7:3 ratio (Fig. 1). The clinical characteristics of the patients were recorded. The SUVmax, mean standardized uptake value (SUVmean), and metabolic tumor volume (MTV) of the primary lesions were measured semi-automatically using the Advanced Workstation (AW, version 4.5, GE Healthcare), whereas the total lesion glycolysis (TLG) was calculated using a formula (TLG = SUVmean x MTV) [22].

EGFR Mutational Status

Tumor tissue specimens were obtained via biopsy or surgical resection and tested using real-time fluorescence quantitative polymerase chain reaction. If accompanied by mutations in any EGFR exon 18–21, it was considered an EGFR mutation; otherwise, it was considered a wild-type EGFR.

FDG PET/CT Image Acquisition

Patients fasted for more than 6 hours before the examination and had a blood glucose level of < 11.10 mmol/L. An intravenous injection of ^{18}F-FDG (0.10–0.15 mCi/kg) was administered, followed by approximately 1 hour of rest. All patients were positioned supine on the GE Discovery Elite PET/CT couch and scanned from the cranial

https://doi.org/10.3348/kjr.2022.0295

Korean Journal of Radiology
KJR

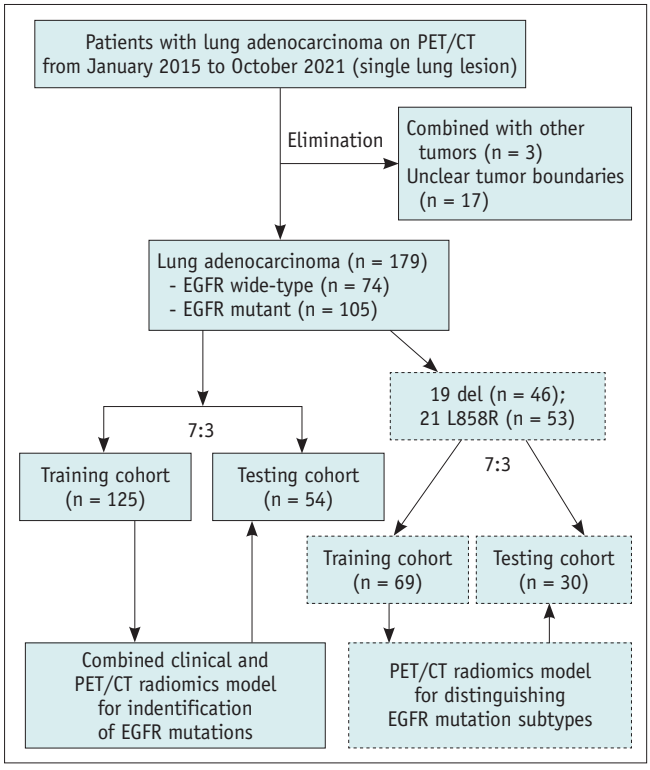

Fig. 1. The flowchart of the study participants. EGFR = epidermal growth factor receptor, 19 del = 19 deletion, 21 L858R = 21 L858R missense

vault to the mid-femoral level. The detailed scanning plan and parameters were as follows. A spiral CT scan was performed under 140 kV tube voltage, 180–240 mA automatic tube current, and 3.75 mm slice thickness. According to the patients' height, PET images were acquired in 6–7 beds, and each bed position took 1.5 minutes. PET images were attenuated by CT data and reconstructed using a three-dimensional ordered subset expectation-maximization algorithm.

Image Pre-Processing, ROI Segmentation, and Feature Extraction

Image pre-processing was completed using the Artificial Intelligence Kit (A.K, version 3.2.0, GE Healthcare), and followed the Image Biomarker Standardization Initiative guidelines [23]. The transverse thickness of CT images was resampled to 1 mm by using a linear interpolation algorithm as well as coronal and sagittal sections. The CT image normalization was accomplished by Gaussian filtering. Only image standardization was required for the pre-processing of PET images. After image pre-processing, the ROIs from the CT and PET images were separately segmented by two experienced nuclear medicine physicians using ITK-SNAP (version 3.8, http://www.itksnap.org/pmwiki/pmwiki.php). They adopted a combination of manual and semi-automatic (adaptive brush tool) methods to delineate the tumor boundaries layer by layer. Eventually, the ROI did not include calcifications, vacuoles, or normal lung tissue. Neither physician was aware of the patient's EGFR mutations.

The radiomics features were automatically calculated and extracted with the utilization of A.K. The radiomics features of the original images included 18 first-order features, 14 shape features, 24 gray level co-occurrence matrix features, 14 gray level dependence matrix features, 16 gray level run-length matrix features, 16 gray level size zone matrix, and five neighboring gray tone difference matrix features. Subsequently, filters, including wavelet, local binary pattern, and Laplacian of Gaussian, were applied to the original PET and CT images to obtain more efficient features (except shape features). Finally, 1316 x 2 radiomics features were extracted from the PET and CT images.

Modeling for Identification of EGFR Mutations

Radiomics feature screening was performed using IPM statistics (IPMs, version 2.5.2, GE Healthcare). First, we adopted variance to select the 2632 PET/CT radiomics features (threshold: 1.0). Further, 1070 radiomics features were retained. However, some of them had a strong linear relationship with each other. Hence, the correlation selection method (Correlation_xx) was utilized to remove features with correlations greater than 0.7 between independent variables, and 176 radiomics features remained. Subsequently, optimal feature subset selection was performed using univariable logistic regression analysis ($p < 0.050$) and multivariable logistic regression analysis (p-in < 0.050, p-out > 0.100) using a stepwise selection method. A radiomics model score (rad-score) was built based on the optimal feature subsets, and the PET/CT radiomics model, whose parameters were determined by a 5-fold cross-validation method, was constructed using logistic regression. Receiver operating characteristic (ROC) curve analysis was performed to determine the performance of the PET/CT radiomics model in the training and testing cohorts. Similarly, we established CT and PET radiomics models.

To integrate PET/CT radiomics and clinical features, we constructed a combined diagnostic model based on the rad-score with the addition of sex, smoking history, and tumor diameter using a multivariable logistic regression model.

https://doi.org/10.3348/kjr.2022.0295

Moreover, a clinical diagnosis model was built based on the tumor diameter, sex, and smoking history.

Modeling to Differentiate EGFR Mutational Subtypes

There were 46 patients with 19 del mutations and 53 with 21 L858R mutations. The patients were divided into training and testing cohorts (69:30). The optimal radiomics feature subsets of PET/CT were screened using Pearson's correlation analysis (cutoff: 0.7) and univariable analysis ($p < 0.050$). A PET/CT radiomics model for discriminating EGFR mutational subtypes was constructed on the subsets, and the performance of the model was assessed using ROC curve analyses.

Statistical Analysis

All statistical analyses were performed using IPMs or SPSS 25.0 (IBM Corp.). Independent sample *t* tests or Mann–Whitney U tests were used for continuous variables, and categorical variables were tested using the χ^2 or Fisher exact probability method. The Delong test was used to assess the statistical differences in the area under the ROC curve (AUROC) of the models. A two-tailed test with $p < 0.050$ was considered statistically significant.

RESULTS

Characteristics of the Patients

Table 1 shows the characteristics of the 179 patients. Smoking history was significantly different between those with EGFR wild-type and EGFR mutations in both the training ($p = 0.001$) and testing cohorts ($p < 0.001$), whereas there were no statistical differences in terms of age, SUVmax, or SUVmean between EGFR mutation and EGFR wild-type (all $p > 0.050$). Female were more likely to have EGFR mutations in the training cohort ($p = 0.001$), while in the testing cohort, the difference was not statistically significant ($p = 0.074$). Compared to those of the wild-type, the MTV and TLG of the EGFR mutation were lower; however, the differences were not statistically significant in the training cohort ($p = 0.056$ and $p = 0.051$, respectively).

Feature Selection in the PET/CT, PET, and CT Radiomics Models

The optimal feature subsets for the PET/CT radiomics model contained four CT and two PET radiomics features (Supplementary Table 1). The rad-score was calculated based on these six features using the following formula: rad-score = 0.55745595 - 0.56643332 x CT-HHL + 1.17316734 x CT-glszm - 1.04555703 x CT-lbp - 0.80138451 x PET-HHH - 0.90487447 x CT-LLH + 0.53307567 x PET-lbp. As shown in Figure 2, the rad-scores were significantly different between EGFR mutation and wild-type EGFR in both the training and testing cohorts (both $p < 0.001$). Meanwhile, the CT-glszm of the EGFR mutation was significantly higher than that of the wild-type EGFR (0.35 [0.30, 0.43] vs. 0.30 [0.26, 0.37], $p = 0.001$, Supplementary Table 1). In addition, the PET

Table 1. Patient Characteristics

Characteristics	Training Cohort (n = 125)		*P*	Testing Cohort (n = 54)		*P*
	EGFR Wild-Type (n = 52)	EGFR Mutant (n = 73)		EGFR Wild-Type (n = 22)	EGFR Mutant (n = 32)	
Age, year	59.00 (53.45, 64.00)	60.00 (53.00, 66.30)	0.606	60.05 ± 8.05	62.97 ± 8.81	0.220
Sex			< 0.001			0.074
Male	35	26		9	6	
Female	17	47		13	26	
Smoking history			0.001			< 0.001
Never	24	55		8	27	
Ever or current	28	18		14	5	
Diameter, cm	3.30 (2.40, 4.50)	3.00 (1.97, 3.90)	0.080	3.65 (2.10, 4.71)	2.25 (1.84, 2.81)	0.033
SUVmax	12.18 (9.73, 15.01)	11.01 (7.88, 15.46)	0.136	13.86 (9.31, 17.54)	10.95 (5.98, 13.22)	0.065
SUVmean	7.39 (5.77, 9.13)	6.70 (4.73, 9.37)	0.217	8.72 (5.69, 10.71)	6.48 (3.61, 8.02)	0.098
MTV	8.68 (4.57, 20.53)	5.87 (2.33, 12.35)	0.056	7.98 (3.88, 17.97)	3.06 (1.75, 7.30)	0.023
TLG	59.73 (31.45, 158.02)	43.50 (11.95, 108.24)	0.051	86.48 (16.92, 164.40)	21.02 (8.27, 53.33)	0.027
Rad-score	-1.05 ± 1.98	1.70 ± 1.83	< 0.001	-0.88 ± 2.27	1.79 ± 2.25	< 0.001

Data are median (interquartile range) or mean ± standard deviation for continuous variables and patient numbers for categorical variables. EGFR = epidermal growth factor receptor, MTV = metabolic tumor volume, Rad-score = radiomics score, SUVmax = maximum standardized uptake value, SUVmean = mean standardized uptake value, TLG = total lesion glycolysis

https://doi.org/10.3348/kjr.2022.0295

Korean Journal of Radiology
KJR

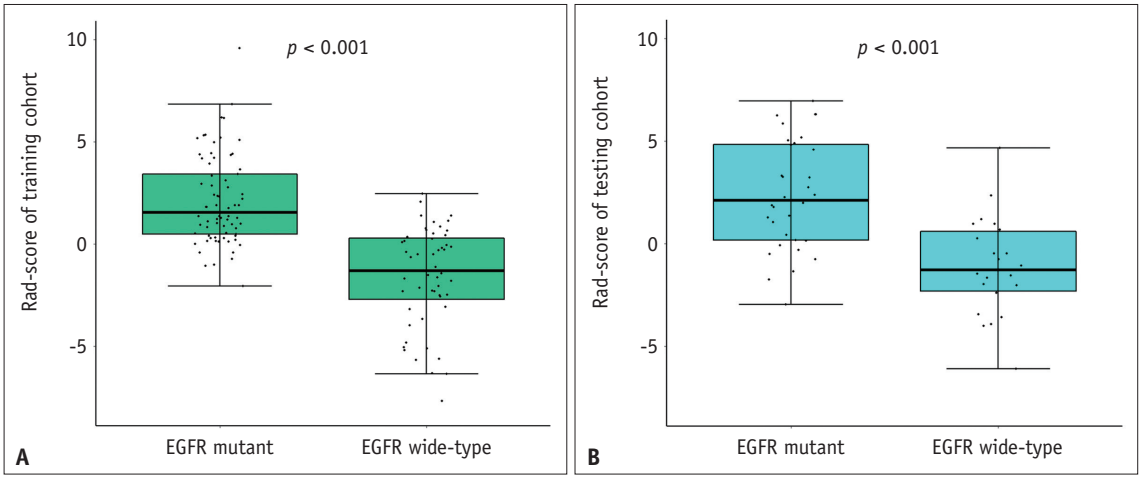

Fig. 2. Distribution of rad-scores.
A. Box plot of rad-score in the training cohort. **B.** Box plot of rad-score in the testing cohort. EGFR = epidermal growth factor receptor, rad-score = radiomics score

Table 2. The Diagnostic Performance of Each Model in Identifying EGFR Mutations

Model	AUROC (95% CI)	Accuracy	Sensitivity	Specificity
Training cohort				
Clinical	0.746 (0.672, 0.82)	0.72	0.753	0.673
CT	0.781 (0.711, 0.848)	0.76	0.849	0.635
PET	0.72 (0.643, 0.793)	0.672	0.589	0.788
PET/CT	0.853 (0.794, 0.905)	0.784	0.767	0.808
Combined	0.882 (0.829, 0.927)	0.816	0.904	0.692
Testing cohort				
Clinical	0.737 (0.618, 0.844)	0.667	0.781	0.5
CT	0.78 (0.669, 0.882)	0.722	0.812	0.591
PET	0.717 (0.596, 0.835)	0.685	0.594	0.818
PET/CT	0.804 (0.699, 0.898)	0.741	0.719	0.773
Combined	0.837 (0.746, 0.918)	0.741	0.781	0.682

Accuracy, sensitivity, and specificity are obtained to give the larges Youden index value. AUROC = area under the ROC curve, CI = confidence interval

model was based on two PET radiomics features, and the CT model was established using three CT radiomics features.

Model Performance in Identifying EGFR Mutations

As presented in Table 2, the AUROCs of the PET/CT radiomics model were higher than those of the PET and CT radiomics models in both the training and testing cohorts, albeit mostly without statistical significance (vs. PET, p = 0.019 and p = 0.356, respectively) (vs. CT, p = 0.109, p = 0.797, respectively). The AUROC of PET/CT radiomics for diagnosing the EGFR mutational status was 0.853 in the training cohort, with an accuracy rate of 78.4%. In the testing cohort, these were 0.804 and 74.1%, respectively.

The performance of the clinical diagnostic model was moderate, with AUROCs of 0.746 and 0.737 for the training and testing cohorts, respectively. When PET/CT radiomics and clinical features were integrated, the combined model (Logit(p) = -1.1422 + 1.1439 x rad-score + 0.1707 x tumor diameter + 1.3331 × sex - 0.5200 x smoking history) showed a higher AUROC than that of the PET/CT radiomics model (Fig. 3), albeit without statistical significance (p = 0.145 and p = 0.182 for the training and testing cohorts, respectively). With the combined model, the accuracy in the training cohort increased to 81.6% and the sensitivity in the training and testing cohorts increased to 90.4% and 78.1%, respectively.

Model Performance in Distinguishing EGFR Mutational Subtypes

As shown in Table 3, there were no significant differences in sex, smoking history, tumor diameter, SUVmax, SUVmean, MTV, or TLG between the 19 del and 21 L858R cohorts (all p > 0.050). The EGFR mutational subtype identification model was based on the four PET/CT radiomic features. The AUROCs of the training and testing cohorts were 0.708 and 0.652, respectively, and their accuracies were 66.7% and 56.7%, respectively (Fig. 4).

DISCUSSION

Targeted therapy benefits tumor patients [24,25]. With regard to lung adenocarcinoma, EGFR-TKIs can prolong the survival of patients with EGFR mutations, whereas patients

https://doi.org/10.3348/kjr.2022.0295

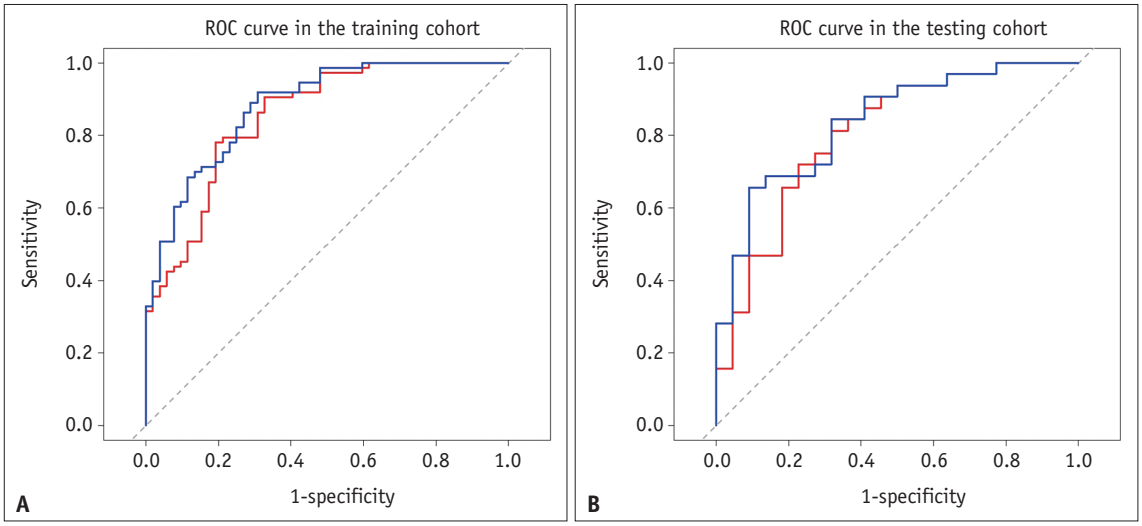

Fig. 3. ROC curves for the PET/CT radiomics (red) and the combined model (blue) for predicting epidermal growth factor receptor mutation in lung adenocarcinoma.
A. ROC curve of the training cohort (AUROC: 0.853 vs. 0.882, $p = 0.145$). **B.** ROC curve of the testing cohort (AUROC: 0.804 vs. 0.837, $p = 0.182$). AUROC = area under the ROC curve, ROC = receiver operating characteristic

Table 3. Characteristics of 19 del and 21 L858R Subsample

Characteristics	Training Cohort (n = 69)		*P*	Testing Cohort (n = 30)		*P*
	19 del (n = 32)	21 L858R (n = 37)		19 del (n = 14)	21 L858R (n = 16)	
Age, year	59.09 ± 9.47	62.97 ± 9.02	0.086	60.00 ± 11.31	60.44 ± 6.46	0.896
Sex			0.497			0.442
Male	8	12		6	4	
Female	24	25		8	12	
Smoking history			0.980			0.072
Never	25	29		9	15	
Ever or current	7	8		5	1	
Diameter, cm	3.00 (1.99, 3.67)	2.60 (1.97, 4.06)	0.764	2.65 (1.80, 3.21)	2.30 (1.65, 3.10)	0.442
SUVmax	11.06 (7.82, 13.33)	11.45 (7.65, 14.27)	0.773	11.73 ± 6.38	9.44 ± 4.48	0.272
SUVmean	6.70 (4.59, 8.09)	7.17 (4.73, 8.92)	0.764	7.27 ± 4.09	5.64 ± 2.59	0.212
MTV	5.28 (2.56, 10.57)	5.17 (1.87, 12.52)	0.691	4.89 (2.63, 10.89)	3.30 (1.69, 6.92)	0.360
TLG	30.75 (14.18, 94.79)	37.78 (9.23, 91.02)	0.718	29.21 (13.55, 80.90)	13.22 (7.78, 46.19)	0.280

Data are mean ± standard deviation or median (interquartile range) for continuous variables and patient numbers for categorical variables. MTV = metabolic tumor volume, SUVmax = maximum standardized uptake value, SUVmean = mean standardized uptake value, TLG = total lesion glycolysis, 19 del = 19 deletion, 21 L858R = 21 L858R missense

with wild-type EGFR do not benefit significantly. Studies have reported more than 200 types of EGFR mutations, the most prominent of which are 19 del and 21 L858R [26], and the outcome of targeted therapy differs between the two types [27,28]. For more precise individualized treatment, it is necessary to identify whether a lung adenocarcinoma patient has an EGFR mutation as well as the specific subtype of the mutation.

Some researchers have reported that the SUVmax of EGFR mutations is significantly lower than that of the wild-type [29]. However, no statistical difference in the SUVmax was observed between EGFR mutations and wild-type EGFR in our study; the same was found for MTV and TLG in the training cohort (all $p > 0.050$), which is consistent with the findings of Chung [30]. Furthermore, Kanmaz et al. [31] suggested that tumors with higher SUVmax were more likely to have EGFR mutations. This discrepancy might have been caused by the sample characteristics, as only adenocarcinoma patients were enrolled in our study. Furthermore, the selection and measurement method for the ROI also have a certain impact. In summary, PET/CT metabolic parameters may be ineffective for diagnosing the

https://doi.org/10.3348/kjr.2022.0295

Korean Journal of Radiology
KJR

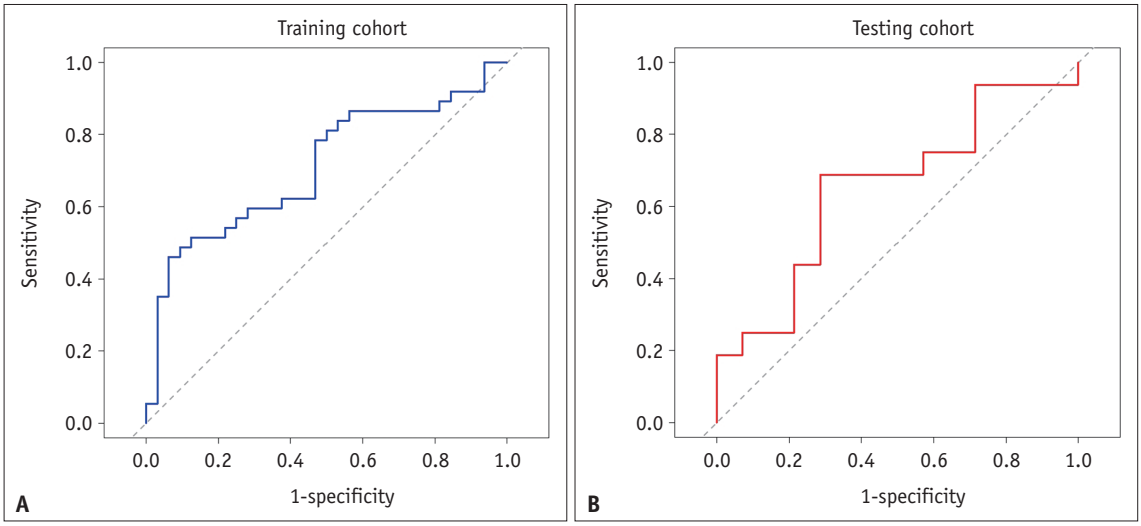

Fig. 4. ROC curves for the PET/CT radiomics model for distinguishing epidermal growth factor receptor mutation subtypes.
A. ROC curve of the training cohort (AUROC: 0.708). **B.** ROC curve of the testing cohort (AUROC: 0.652). AUROC = area under the ROC curve, ROC = receiver operating characteristic

EGFR mutation status. Therefore, we attempted to construct diagnostic models based on PET/CT radiomic features.

The radiomic features of PET/CT can reflect the distribution characteristics of the tumor pixel grayscale and reveal the heterogeneity of the spatial distribution of ^{18}F-FDG within the tumor [32]. In our study, the rad-score was constructed based on the six PET/CT radiomics features. Patients with EGFR wild-type had lower rad-score than those with EGFR mutations in the training and testing cohorts (both $p < 0.001$), which agrees with two other studies [33,34]. Therefore, the rad-score was feasible as a predictor of EGFR mutational status. Furthermore, we found that the CT-glszm of EGFR-mutant tumors was higher ($p = 0.001$), indicating a higher heterogeneity between regional size volumes in images. Zhang et al. [34] also reported that tumors with EGFR mutations were more heterogeneous. Furthermore, comparing the three radiomics models, the PET/CT radiomics model might have been the best, with AUROCs and accuracies of 0.853 and 0.804, and 78.4% and 74.1% in the training and testing cohorts, respectively, although further confirmation in a larger sample is needed. This was consistent with the results reported by Li et al. [20].

The identification of EGFR mutation status using radiomics features alone is one-sided. A previous study showed that female and non-smokers were more likely to have EGFR mutations [35], which is consistent with our results. Moreover, Chang et al. [36] stated that tumors with EGFR mutations were shorter and smaller than those with wild-type EGFR. Therefore, we constructed a combined model by incorporating the rad-score, sex, smoking history, and tumor diameter. Although there was no statistical difference in the AUROCs between the combined and PET/CT radiomics model in both the training and testing cohorts (0.853 vs. 0.882, $p = 0.145$; 0.804 vs. 0.837, $p = 0.182$, respectively). The sensitivity of the training and testing cohorts increased to 90.4% and 78.1%, respectively, and the accuracy improved to 81.6% in the training cohort. Zhang et al. [33] also proved that the combined model was superior to the PET/CT radiomics model; the AUROC and accuracy of the combined model were 0.86 and 80.0% in the training cohort, and 0.87 and 80.8% in the testing cohort, respectively. In another study, Chang et al. [36] demonstrated that an integrated model based on PET/CT radiomics and CT morphological features was better than the PET/CT radiomics model (AUROC, 0.84 vs. 0.76; AUROC, 0.81 vs. 0.75, respectively). However, the identification of morphological features relies on the subjective experience of physicians, which is time consuming and less reproducible. Therefore, we believe that it is feasible and reproducible to identify the EGFR mutational status by combining PET/CT radiomics and clinical features.

The preferred targeting agents for patients with 19 del and 21 L858R mutations differ, in addition to their therapeutic efficacy [37]. We found no statistical differences in sex, smoking history, tumor diameter, SUVmax, SUVmean, MTV, and TLG (all $p > 0.050$) between the 19 del and 21 L858R cohorts, which is consistent with the results of Liu et al. [38]. Therefore, distinguish between

https://doi.org/10.3348/kjr.2022.0295

these two subtypes may be difficult using metabolic or clinical parameters. Liu et al. [38] constructed models based on PET/CT radiomics features to identify wild-type EGFR and 19 del (AUROC, 0.77), and wild-type EGFR and 21 L858R (AUROC, 0.92). However, the authors did not directly compare any difference in PET/CT radiomic features between the two subtypes. Zhang et al. [34] attempted to distinguish 19 del and 21 L858R directly using PET/CT radiomics features, and the data showed that only one feature could be identified with an AUROC and an accuracy of 0.661 and 43.1%, respectively. In our study, we built an EGFR mutational subtype identification model based on PET/CT radiomics with an AUROC and accuracy of 0.708 and 66.7% in the training cohort and 0.652 and 56.7% in the testing cohort, respectively. The performance of the model was poor, implying that it may be difficult to distinguish mutant subtypes directly using PET/CT radiomics. However, the sample size in this study was small, making it difficult to evaluate the usefulness of PET/CT radiomics.

Our study had some limitations. First, in the manual and semi-automatic outlining approaches artificial mistakes are difficult to avoid and are less repeatable compared to fully automatic outlining. Second, external data validation was not performed. Finally, the sample size was small, and a multicenter study with a large sample size is required to further investigate the stability and usefulness of the joint model.

In conclusion, the combined clinical and PET/CT radiomics model constructed by integrating radiomics and clinical features could identify the EGFR mutational status in lung adenocarcinoma with moderate accuracy, which may help non-invasively screen high-risk groups for EGFR mutations in clinical practice. However, it is more challenging to further distinguish EGFR mutational subtypes using PET/CT radiomics.

Supplement

The Supplement is available with this article at https://doi.org/10.3348/kjr.2022.0295.

Availability of Data and Material

The datasets generated or analyzed during the study are available from the corresponding author on reasonable request.

Conflicts of Interest

The authors have no potential conflicts of interest to disclose.

Author Contributions

Conceptualization: Shen Li, Jun Xin. Data curation: Shen Li. Formal analysis: Shen Li, Jun Xin. Investigation: Shen Li, Yadi Li. Methodology: Shen Li, Yadi Li, Min Zhao, Pengyuan Wang. Project administration: Shen Li, Jun Xin. Resources: Shen Li, Jun Xin. Software: Shen Li, Yadi Li, Min Zhao, Pengyuan Wang. Supervision: Jun Xin. Validation: Jun Xin. Writing—original draft: Shen Li. Writing—review & editing: all authors.

ORCID iDs

Shen Li
https://orcid.org/0000-0003-1530-5221
Yadi Li
https://orcid.org/0000-0001-9473-8839
Min Zhao
https://orcid.org/0000-0002-7154-8415
Pengyuan Wang
https://orcid.org/0000-0003-2441-1384
Jun Xin
https://orcid.org/0000-0001-5660-6368

Funding Statement

None

Acknowledgments

The authors thank all their coworkers involved in the study for their support and assistance.

REFERENCES

1. Bray F, Ferlay J, Soerjomataram I, Siegel RL, Torre LA, Jemal A. Global cancer statistics 2018: GLOBOCAN estimates of incidence and mortality worldwide for 36 cancers in 185 countries. *CA Cancer J Clin* 2018;68:394-424
2. Siegel RL, Miller KD, Jemal A. Cancer statistics, 2020. *CA Cancer J Clin* 2020;70:7-30
3. Lortet-Tieulent J, Soerjomataram I, Ferlay J, Rutherford M, Weiderpass E, Bray F. International trends in lung cancer incidence by histological subtype: adenocarcinoma stabilizing in men but still increasing in women. *Lung Cancer* 2014;84:13-22
4. Jia Y, Yun CH, Park E, Ercan D, Manuia M, Juarez J, et al. Overcoming EGFR(T790M) and EGFR(C797S) resistance with

mutant-selective allosteric inhibitors. *Nature* 2016;534:129-132
5. Wu SG, Shih JY. Management of acquired resistance to EGFR TKI-targeted therapy in advanced non-small cell lung cancer. *Mol Cancer* 2018;17:38
6. An N, Zhang Y, Niu H, Li Z, Cai J, Zhao Q, et al. EGFR-TKIs versus taxanes agents in therapy for nonsmall-cell lung cancer patients: a PRISMA-compliant systematic review with meta-analysis and meta-regression. *Medicine (Baltimore)* 2016;95:e5601
7. Cheng H, Li XJ, Wang XJ, Chen ZW, Wang RQ, Zhong HC, et al. A meta-analysis of adjuvant EGFR-TKIs for patients with resected non-small cell lung cancer. *Lung Cancer* 2019;137:7-13
8. Chen RL, Sun LL, Cao Y, Chen HR, Zhou JX, Gu CY, et al. Adjuvant EGFR-TKIs for patients with resected EGFR-mutant non-small cell lung cancer: a meta-analysis of 1,283 patients. *Front Oncol* 2021;11:629394
9. Suda K, Mitsudomi T, Shintani Y, Okami J, Ito H, Ohtsuka T, et al. Clinical impacts of EGFR mutation status: analysis of 5780 surgically resected lung cancer cases. *Ann Thorac Surg* 2021;111:269-276
10. Ellison G, Zhu G, Moulis A, Dearden S, Speake G, McCormack R. EGFR mutation testing in lung cancer: a review of available methods and their use for analysis of tumour tissue and cytology samples. *J Clin Pathol* 2013;66:79-89
11. Zhang Y, Chang L, Yang Y, Fang W, Guan Y, Wu A, et al. Intratumor heterogeneity comparison among different subtypes of non-small-cell lung cancer through multi-region tissue and matched ctDNA sequencing. *Mol Cancer* 2019;18:7
12. Kandathil A, Kay FU, Butt YM, Wachsmann JW, Subramaniam RM. Role of FDG PET/CT in the eighth edition of TNM staging of non–small cell lung cancer. *Radiographics* 2018;38:2134-2149
13. Borggreve AS, Goense L, van Rossum PSN, Heethuis SE, van Hillegersberg R, Lagendijk JJW, et al. Preoperative prediction of pathologic response to neoadjuvant chemoradiotherapy in patients with esophageal cancer using 18F-FDG PET/CT and DW-MRI: a prospective multicenter study. *Int J Radiat Oncol Biol Phys* 2020;106:998-1009
14. Cho A, Hur J, Moon YW, Hong SR, Suh YJ, Kim YJ, et al. Correlation between EGFR gene mutation, cytologic tumor markers, 18F-FDG uptake in non-small cell lung cancer. *BMC Cancer* 2016;16:224
15. Hong IK, Lee JM, Hwang IK, Paik SS, Kim C, Lee SH. Diagnostic and predictive values of 18F-FDG PET/CT metabolic parameters in EGFR-mutated advanced lung adenocarcinoma. *Cancer Manag Res* 2020;12:6453-6465
16. Wang Y, Zhao N, Wu Z, Pan N, Shen X, Liu T, et al. New insight on the correlation of metabolic status on 18F-FDG PET/CT with immune marker expression in patients with non-small cell lung cancer. *Eur J Nucl Med Mol Imaging* 2020;47:1127-1136
17. Caicedo C, Garcia-Velloso MJ, Lozano MD, Labiano T, Vigil Diaz C, Lopez-Picazo JM, et al. Role of [18F]FDG PET in prediction of KRAS and EGFR mutation status in patients with advanced non-small-cell lung cancer. *Eur J Nucl Med Mol Imaging* 2014;41:2058-2065
18. Krarup MMK, Nygård L, Vogelius IR, Andersen FL, Cook G, Goh V, et al. Heterogeneity in tumours: validating the use of radiomic features on 18F-FDG PET/CT scans of lung cancer patients as a prognostic tool. *Radiother Oncol* 2020;144:72-78
19. Tu W, Sun G, Fan L, Wang Y, Xia Y, Guan Y, et al. Radiomics signature: a potential and incremental predictor for EGFR mutation status in NSCLC patients, comparison with CT morphology. *Lung Cancer* 2019;132:28-35
20. Li X, Yin G, Zhang Y, Dai D, Liu J, Chen P, et al. Predictive power of a radiomic signature based on 18F-FDG PET/CT images for EGFR mutational status in NSCLC. *Front Oncol* 2019;9:1062
21. Koyasu S, Nishio M, Isoda H, Nakamoto Y, Togashi K. Usefulness of gradient tree boosting for predicting histological subtype and EGFR mutation status of non-small cell lung cancer on 18F FDG-PET/CT. *Ann Nucl Med* 2020;34:49-57
22. Yang B, Wang QG, Lu M, Ge Y, Zheng YJ, Zhu H, et al. Correlations study between 18F-FDG PET/CT metabolic parameters predicting epidermal growth factor receptor mutation status and prognosis in lung adenocarcinoma. *Front Oncol* 2019;9:589
23. Zwanenburg A, Vallières M, Abdalah MA, Aerts HJWL, Andrearczyk V, Apte A, et al. The image biomarker standardization initiative: standardized quantitative radiomics for high-throughput image-based phenotyping. *Radiology* 2020;295:328-338
24. Solomon BJ, Mok T, Kim DW, Wu YL, Nakagawa K, Mekhail T, et al. First-line crizotinib versus chemotherapy in ALK-positive lung cancer. *N Engl J Med* 2014;371:2167-2177
25. Passaro A, Prelaj A, Bonanno L, Tiseo M, Tuzi A, Proto C, et al. Activity of EGFR TKIs in Caucasian patients with NSCLC harboring potentially sensitive uncommon EGFR mutations. *Clin Lung Cancer* 2019;20:e186-e194
26. Castellanos E, Feld E, Horn L. Driven by mutations: the predictive value of mutation subtype in EGFR-mutated non-small cell lung cancer. *J Thorac Oncol* 2017;12:612-623
27. Li WQ, Cui JW. Non-small cell lung cancer patients with ex19del or exon 21 L858R mutation: distinct mechanisms, different efficacies to treatments. *J Cancer Res Clin Oncol* 2020;146:2329-2338
28. Hong W, Wu Q, Zhang J, Zhou Y. Prognostic value of EGFR 19-del and 21-L858R mutations in patients with non-small cell lung cancer. *Oncol Lett* 2019;18:3887-3895
29. Yip SS, Kim J, Coroller TP, Parmar C, Velazquez ER, Huynh E, et al. Associations between somatic mutations and metabolic imaging phenotypes in non-small cell lung cancer. *J Nucl Med* 2017;58:569-576
30. Chung HW, Lee KY, Kim HJ, Kim WS, So Y. FDG PET/CT metabolic tumor volume and total lesion glycolysis predict

prognosis in patients with advanced lung adenocarcinoma. *J Cancer Res Clin Oncol* 2014;140:89-98
31. Kanmaz ZD, Aras G, Tuncay E, Bahadır A, Kocatürk C, Yaşar ZA, et al. Contribution of 18Fluorodeoxyglucose positron emission tomography uptake and TTF-1 expression in the evaluation of the EGFR mutation in patients with lung adenocarcinoma. *Cancer Biomark* 2016;16:489-498
32. Chicklore S, Goh V, Siddique M, Roy A, Marsden PK, Cook GJ. Quantifying tumour heterogeneity in 18F-FDG PET/CT imaging by texture analysis. *Eur J Nucl Med Mol Imaging* 2013;40:133-140
33. Zhang J, Zhao X, Zhao Y, Zhang J, Zhang Z, Wang J, et al. Value of pre-therapy 18F-FDG PET/CT radiomics in predicting EGFR mutation status in patients with non-small cell lung cancer. *Eur J Nucl Med Mol Imaging* 2020;47:1137-1146
34. Zhang M, Bao Y, Rui W, Shangguan C, Liu J, Xu J, et al. Performance of 18F-FDG PET/CT radiomics for predicting EGFR mutation status in patients with non-small cell lung cancer. *Front Oncol* 2020;10:568857
35. Kosaka T, Yatabe Y, Endoh H, Kuwano H, Takahashi T, Mitsudomi T. Mutations of the epidermal growth factor receptor gene in lung cancer: biological and clinical implications. *Cancer Res* 2004;64:8919-8923
36. Chang C, Zhou S, Yu H, Zhao W, Ge Y, Duan S, et al. A clinically practical radiomics-clinical combined model based on PET/CT data and nomogram predicts EGFR mutation in lung adenocarcinoma. *Eur Radiol* 2021;31:6259-6268
37. Sutiman N, Tan SW, Tan EH, Lim WT, Kanesvaran R, Ng QS, et al. EGFR mutation subtypes influence survival outcomes following first-line gefitinib therapy in advanced Asian NSCLC patients. *J Thorac Oncol* 2017;12:529-538
38. Liu Q, Sun D, Li N, Kim J, Feng D, Huang G, et al. Predicting EGFR mutation subtypes in lung adenocarcinoma using 18F-FDG PET/CT radiomic features. *Transl Lung Cancer Res* 2020;9:549-562

https://doi.org/10.3348/kjr.2022.0295